

A. V. Pimikov\* · S. V. Mikhailov · N. G. Stefanis

# Rho meson distribution amplitudes from QCD sum rules with nonlocal condensates

Received: date / Accepted: date

**Abstract** The leading-twist distribution amplitude for the longitudinal rho-meson was studied using QCD Sum Rules with nonlocal condensates and a spectral density which includes next-to-leading order radiative corrections. The obtained profile is compared with results from standard QCD sum rules, lattice QCD, holographic QCD, a light-front quark model, and the instanton liquid model. Preliminary estimates for the first two moments of the transverse  $\rho$ -meson distribution amplitude are also given.

**Keywords** Rho-meson properties · Meson Distribution Amplitudes · QCD Sum Rules

## 1 Introduction

The knowledge of the partonic  $\rho$ -meson structure is very important for the theoretical description of different hard exclusive processes, such as the B-meson decays ( $B \rightarrow \rho l \nu$ ,  $\overline{B}^0 \rightarrow \rho^0 \gamma$ ) [1; 2], the  $\rho$ -meson electro-photoproduction [3], and the determination of the Cabibbo–Kobayashi–Maskawa matrix element  $|V_{ub}|$  [1]. In this report, we focus on the construction of the leading-twist distribution amplitude (DA),  $\varphi_\rho^L(x, \mu^2)$ , for the longitudinal  $\rho$  meson, defined by

$$\langle 0 | \bar{d}(z) \gamma_\mu u(0) | \rho(p, \lambda) \rangle \Big|_{z^2=0} = f_\rho p_\mu \int_0^1 dx e^{ix(z \cdot p)} \varphi_\rho^L(x, \mu^2). \quad (1)$$

On the other hand, the transverse  $\rho$ -meson DA,  $\varphi_\rho^T(x, \mu^2)$ , is given by

$$\langle 0 | \bar{d}(z) \sigma_{\mu\nu} u(0) | \rho(p, \lambda) \rangle \Big|_{z^2=0} = i f_\rho^T (\varepsilon_\mu^{(\lambda)} p_\nu - \varepsilon_\nu^{(\lambda)} p_\mu) \int_0^1 dx e^{ix(z \cdot p)} \varphi_\rho^T(x, \mu^2), \quad (2)$$

where  $p_\nu$  and  $\varepsilon_\mu^{(\lambda)}$  are the momentum and polarization vector of the  $\rho$  meson, respectively, and  $\mu^2$  is the normalization point. A fuller description of this DA will be given in a separate publication. Here, we will

---

\* Presented by the first author at the Light-Cone Conference 2013, May 20-24, 2013, Skiathos, Greece.

A. V. Pimikov  
 Departamento de Física Teórica -IFIC, Universidad de Valencia-CSIC, E-46100 Burjassot (Valencia), Spain  
 Bogoliubov Laboratory of Theoretical Physics, JINR, 141980 Dubna, Russia  
 E-mail: alexandr.pimikov@uv.es

S. V. Mikhailov  
 Bogoliubov Laboratory of Theoretical Physics, JINR, 141980 Dubna, Russia  
 E-mail: mikhs@theor.jinr.ru

N. G. Stefanis  
 Institut für Theoretische Physik II, Ruhr-Universität Bochum, D-44780 Bochum, Germany  
 E-mail: stefanis@tp2.ruhr-uni-bochum.de

only present preliminary estimates for its first two moments. The evolution with the factorization scale  $\mu^2$  of the  $\varphi_\rho^L(x, \mu^2)$  and  $\varphi_\pi(x, \mu^2)$  DAs is taken into account by means of the Efremov–Radyushkin–Brodsky–Lepage evolution equation [4; 5]. Note that the next-to-leading order (NLO) evolution of  $\varphi_\rho^L(x, \mu^2)$  resembles that of  $\varphi_\pi(x, \mu^2)$  — see, e.g., [6].

The  $\rho_{(L,T)}$ -meson DAs (longitudinal and transverse) were first constructed within the standard QCD SR approach [7; 8], which employs local condensates. Their determination within the framework of QCD SRs with nonlocal condensates (NLC) was considered later in [9; 10; 11]. Besides, the  $\rho$ -meson DAs were studied in other nonperturbative approaches as well, e.g., lattice QCD [12], AdS/QCD holography [13; 14; 2; 3], the light-front quark model [15], and the instanton liquid model [16]. In this note we improve the previous works in [9; 10; 11] on the  $\rho$ -meson longitudinal and transverse DAs in the following respects: (i) we use a corrected expression for the NLO spectral density in the SR for the  $\rho_L$  DA, (ii) we express the  $\rho_L$  DA in terms of Gegenbauer coefficients, and (iii) we calculate and use the correct nonperturbative term for the theoretical part of the SR for the  $\rho_T$  DA. We utilize the latter improvement to derive some preliminary estimates for the decay constant and the two lowest-order moments of the  $\rho_T$ -meson DA.

## 2 Distribution amplitudes for the $\rho$ -meson from QCD sum rules with nonlocal condensates

The derivation of the  $\rho$ -meson longitudinal DA is based on the correlator of two vector currents that leads to the following sum rule for the  $\rho$ -DA  $\varphi_\rho^L(x)$ :

$$f_\rho^2 \varphi_\rho^L(x) e^{-m_\rho^2/M^2} + f_{\rho'}^2 \varphi_{\rho'}^L(x) e^{-m_{\rho'}^2/M^2} = \int_0^{s_0} \rho_{\text{pert}}(s, x) e^{-s/M^2} ds + \Phi_\rho(x, M^2), \quad (3a)$$

$$\Phi_{\rho(\pi)}(x, M^2) = \mp \Phi_{4Q}(x, M^2) + \Phi_{\bar{q}Aq}(x, M^2) + \Phi_V(x, M^2) + \Phi_G(x, M^2). \quad (3b)$$

Here,  $M^2$  is the Borel parameter,  $s_0$  denotes the threshold value, and the nonperturbative contribution  $\Phi_\rho$  to the operator product expansion (OPE) contains the following terms:  $\Phi_{4Q}$  (four-quark condensate),  $\Phi_{\bar{q}Aq}$  (quark-gluon-quark condensate),  $\Phi_V$  (vector quark condensate),  $\Phi_G$  (gluon condensate). Note that the r.h.s. of the analogous sum rule for the pion DA receives the same nonperturbative contributions, but has a positive sign in front of the dominant term  $\Phi_{4Q}$  determined by the scalar quark condensate [9].<sup>1</sup> We will discuss later the implications of this sign difference. All these nonperturbative contributions contain nonlocal condensates [17; 18], meaning that the quarks (gluons) in the vacuum can be correlated within distances of the order of  $\Lambda = 1/\lambda_q$  ( $1/\lambda_G$ ). The value of this length scale is fixed by the nonzero average virtuality of the quark fields in the vacuum condensate,  $\lambda_q^2 \equiv \langle \bar{q} D^2 q \rangle / \langle \bar{q} q \rangle$ , which is the only mass-scale setting parameter used to parameterize the nonlocality of the nonperturbative vacuum. A natural and simple ansatz for the spatial ( $z^2 < 0$ ) behavior of the scalar quark condensate is given by a Gaussian model, e.g.,  $\langle \bar{q}(z) q(0) \rangle \sim \exp[z^2 \lambda_q^2 / 8]$  [17; 18] with  $\lambda_q^2 = 0.4 \pm 0.05 \text{ GeV}^2$  [19; 20].

Due to the nonlocality, the behavior of  $\Phi_{\rho(\pi)}(x, M^2)$  becomes less singular with respect to  $x$ . For instance,  $\Phi_{4Q}(x, M^2)$  in Eq. (3b) shows a linear behavior in the vicinity of the endpoints — in contrast to the singular  $\delta(x)$ -behavior in the standard, i.e., local, approach,

$$\Phi_{4Q} \sim x\theta(\Delta - x) \xrightarrow{\lambda_q^2 \rightarrow 0} \Phi_{4Q}^{\text{local}} \sim \delta(x),$$

where  $\Delta = \lambda_q^2 / (2M^2) \in [0.1, 0.3]$ . In order to reduce the model dependence, introduced via the nonlocality ansatz, we study the sum rules for the integral characteristics of the meson DAs, such as the moments  $\langle \xi^N \rangle \equiv \int_0^1 dx \varphi(x) (1 - 2x)^N$  and the inverse moment  $\langle x^{-1} \rangle \equiv \int_0^1 dx \varphi(x) / x$ . In fact, the nonlocal approach gives the opportunity to study the slope  $\varphi'(x \rightarrow 0)$  [21] and the inverse moment  $\langle x^{-1} \rangle$  [22] of the meson DAs. These characteristics are inaccessible when one uses local condensates because of the appearance of non-integrable singularities.

<sup>1</sup> The generic form of the sum rule [10; 11] for the transverse  $\rho_T$  DA, used in our analysis, is similar to (3a) (apart from the appearance on the l.h.s. of the masses of  $\rho$  and  $\rho'$ ).

Following [22], we construct  $\varphi_\rho^L(x, \mu^2)$  in terms of the first few Gegenbauer coefficients which we extract from the moments of the  $\rho_L$  DA, viz.,  $\langle \xi^{2N} \rangle$  with  $N = 0, 1, \dots, 5$ . The moments themselves are determined by evaluating the sum rules in Eq. (3). The obtained results are displayed in Tab. 1. Still higher Gegenbauer coefficients can be set equal to zero, i.e.,  $a_{n \geq 6} = 0$  — a reasonable approximation in view of the closeness of the higher moments to their asymptotic values, cf. the entries in the first and the fourth row of Tab. 1.

**Table 1** Results for the moments of various  $\rho$ -meson DAs derived in our present analysis employing QCD sum rules with nonlocal condensates — cf. Eq. (3). The normalization scale is taken to be  $\mu^2 \approx 1 \text{ GeV}^2$ . The analogous results for the asymptotic DA and the pion DA from Ref. [22] are also given for comparison.

Meson DA	$f_M$	$\langle \xi^2 \rangle$	$\langle \xi^4 \rangle$	$\langle \xi^6 \rangle$	$\langle \xi^8 \rangle$	$\langle \xi^{10} \rangle$	$\langle x^{-1} \rangle_{\text{SR}}$
Asy	1	0.2	0.0857	0.0476	0.030	0.0209	3
$\pi$ [22]	0.137(8)	0.266(20)	0.115(11)	0.060(7)	0.036(5)	0.025(4)	3.35(30)
$\rho_L$ [9]	0.201(5)	0.227(7)	0.095(5)	0.051(4)	0.030(2)	0.020(5)	3.1(1)
$\rho_L$ (here)	0.21(2)	0.216(21)	0.089(9)	0.048(5)	0.030(3)	0.022(2)	3.16(30)
$\rho'_L$ (here)	0.181(26)	0.273(65)	0.175(30)	0.120(17)	0.083(12)	0.058(8)	4(1)
$\rho_T$ (here)	0.169(15)	0.107(11)	0.022(2)	—	—	—	—

The evaluation of the SR in Eq. (3) from the numerical viewpoint is carried out at the scale  $\mu^2 \approx 1 \text{ GeV}^2$  in the following way. For the masses of the  $\rho$ -mesons we use their physical values from [23], i.e.,  $m_\rho = 0.775 \text{ GeV}$ ,  $m_{\rho'} = 1.496 \text{ GeV}$ , and  $m_{\rho''} = 1.72 \text{ GeV}$ . The size of the nonlocality parameter  $\lambda_q^2$  was determined in the analysis of the pion DA, carried out in [22; 24; 19] and was found to be  $\lambda_q^2 = 0.4 \text{ GeV}^2$ . (We ignore here for simplicity its uncertainties, mentioned above.) The coupling constant has the value  $\alpha_s(1 \text{ GeV}^2) = 0.56$ , whereas the quark condensate and the gluon condensate are given by  $\alpha_s \langle \bar{q}q \rangle^2 = 0.000183 \text{ GeV}^6$  and  $\alpha_s \langle GG \rangle / \pi = 0.012 \text{ GeV}^4$ , respectively. The sum rule in (3) was found to be quite stable in a wide range of the threshold parameter  $s_0$ , allowing its variation around the central value  $s_0 = (m_{\rho'}^2 + m_{\rho''}^2)/2$  within the admissible interval of masses  $[m_{\rho'}^2, m_{\rho''}^2]$ . The central values of the decay constant and the moments of the  $\rho'$ -meson depend stronger on the threshold  $s_0$  than the  $\rho$ -meson ground-state values. This leads to a significant increase of the uncertainties of the characteristics of the excited  $\rho'$ -meson state — see Table 1. This table collects the main results of our analysis for  $\rho_L$ ,  $\rho'_L$ , and  $\rho_T$  in terms of the meson decay constants, the first five moments, and the inverse moment of the corresponding DAs. The first two Gegenbauer coefficients of the  $\rho_L$  and the  $\rho'_L$  DA are given in Table 2. In both tables, we also include the previous estimates for  $\rho_L$  from [9] and the corresponding values of the asymptotic DA (abbreviated by Asy), as well as the BMS pion DA derived in [22]. The displayed errors in the parenthesis denote the sum of the uncertainties related to the variation of the threshold parameter  $s_0$ , the normalization constants  $f_\rho$  and  $f'_\rho$ , and the maximal deviation from the average value of the Borel parameter  $M^2$  in its fiducial window:  $M^2 \in [0.6, 2] \text{ GeV}^2$ . Note in passing that an analogous analysis for the pion was carried out in [22] providing reliable results. An obvious observation from Table 1 is that the new estimates for  $\rho_L$  and the older results from [9] are more or less compatible to each other. In contrast, our new estimates for  $\rho_T$  significantly differ from those for the  $\rho_L$  DA. They also disagree with those derived in previous QCD SR approaches [7; 8; 10; 11; 25], or were obtained by other ways in [15; 16]. It is worth mentioning in this context that also the  $x$  behavior of the valence parton distribution functions for  $\rho_T$  and  $\rho_L$ , extracted from QCD SR calculations in [26; 27], turns out to be quite different.

Relying for simplicity only upon the first two Gegenbauer harmonics, we attempt to model the  $\varphi_\rho^L(x, \mu^2)$  meson DA, in terms of the Gegenbauer coefficients  $a_2 = 0.047 \pm 0.058$  and  $a_4 = -0.057 \pm 0.118$  which we determine by means of the first three moments given in Table 1 at the scale  $\mu^2 \approx 1 \text{ GeV}^2$ . The results are given in Table 2 together with the coefficients of the DA of the  $\rho'$  meson determined in this work. For the sake of comparison, we also display the results obtained with the Bakulev–Mikhailov–Stefans (BMS)  $\pi$  DA [22]. Inspection of the displayed values shows that these simple models for the pion and the  $\rho_L$  meson are in good mutual agreement, thus reproducing the observations we made above with respect to the analysis of the QCD sum rules — cf. Table 1.

The evaluation of the SR in (3) leads to a whole set of admissible  $\rho_L$  DAs, as illustrated in the left panel of Fig. 1 in terms of a (blue) shaded “band”. To anticipate the particular characteristics of these

**Table 2** Gegenbauer coefficients and slope  $\varphi'(0)$  of various  $\rho$ -meson DAs, determined at the scale  $\mu^2 \approx 1 \text{ GeV}^2$  with QCD SRs employing nonlocal condensates, cf. (3). In all entries we use  $a_6 = 0$ . The values of the inverse moment  $\langle x^{-1} \rangle_{\text{model}}$  here, in contrast to Table 1, were computed with the aid of DA models based on expansions over two Gegenbauer coefficients.

Model DA	$f_M$	$a_2$	$a_4$	$\varphi'(0)$	$\langle x^{-1} \rangle_{\text{model}}$
Asy	1	0	0	6	3
$\pi$ [22]	0.137(8)	0.187(60)	-0.129(40)	$2 \pm 6$	3.2(1)
$\rho_L$ [9]	0.201(5)	0.079(20)	-0.074(60)	$2 \pm 5$	3.0(1)
$\rho_L$ (here)	0.21(2)	0.047(58)	-0.057(118)	$3 \pm 8$	3.0(2)
$\rho'_L$ (here)	0.169(15)	0.21(19)	0.33(39)	—	—

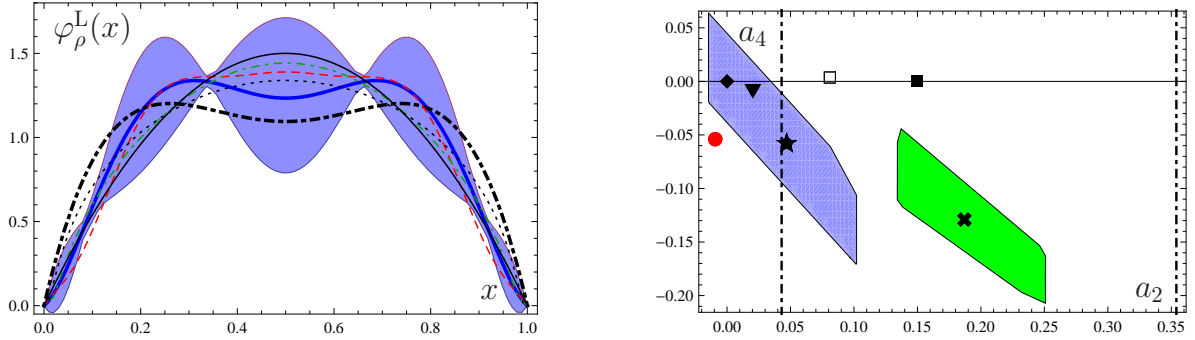


**Fig. 1** Model distribution amplitudes for the longitudinal  $\rho$ -meson (left panel) and their representations in the plane of the Gegenbauer coefficients  $a_2$  and  $a_4$  (right panel). The (blue) shaded areas in both panels indicate the regions of the shape variation admitted by our present analysis based on QCD SRs with nonlocal condensates. The thick solid line inside the DA band corresponds to our optimum  $\rho_L$  DA marked by a  $\star$  in the  $a_2, a_4$  plane. The designations for the other DAs in the right panel are as follows: asymptotic DA (solid thin line,  $\blacklozenge$ ), QCD SRs [25] (thick dashed-dotted line,  $\blacksquare$ ), AdS QCD [2] (dotted line,  $\square$ ), light-front quark model [15] (thin dashed-dotted line,  $\blacktriangledown$ ), instanton liquid model [16] (red dashed line,  $\bullet$ ), and lattice QCD [12] (shown only on the right panel by two vertical broken lines) that indicate the constraints obtained for  $a_2$ . For comparison, we have displayed in the right panel also the area of  $a_2, a_4$  values (green slanted rectangle) determined with QCD SR and NLC in [22] for the pion DA. The BMS model is denoted by the symbol  $\times$  — see for details [22; 28]. All models shown were evolved to  $\mu^2 = 1 \text{ GeV}^2$ , if they were originally determined at another scale.

DAs, we also show the profiles of other models, proposed in the literature, with further explanations provided in the figure caption. The corresponding pairs of Gegenbauer coefficients  $a_2, a_4$  of these model DAs, are displayed in the right panel of this figure. In the plane spanned by the coefficients  $a_2$  and  $a_4$ , the admissible pairs of values, determined in our analysis, appear in the form of a slanted (blue) rectangle, within which the symbol  $\star$  marks the position of the optimum values in satisfying the SR. This particular  $\rho_L$  DA corresponds to the (blue) solid line within the shaded band on the left. The designations of the symbols in the right panel of this figure are defined in the figure caption. For the sake of comparison, we also show the admissible  $a_2, a_4$  set for the pion determined in [22] (green shaded area further to the right). One spots immediately some important differences between the  $\pi$  and the  $\rho_L$  mesons: First, the confidence region for the longitudinal  $\rho$ -meson DA, i.e., the (blue) slanted rectangle, is located closer to the origin (and the asymptotic DA), while, second,  $a_4$  can have positive values as well.

It is instructive to compare the results for the  $\varphi_\rho^L(x, \mu^2)$  DA with their counterparts for  $\varphi_\pi(x, \mu^2)$  in more detail, the goal being to clarify the role of the four-quark contribution  $\Phi_{4Q}$  in the evaluation of the SRs given by (3). The point is that just this condensate contribution enters both SRs, those for the pion and those for the  $\rho$  (see Eq. (3)), but with opposite signs. In the  $\rho$  case, it reduces the total condensate contribution to the SR because it has the opposite sign relative to the other terms. No such cancellation occurs in the pion case. Therefore, the relative weight of  $\Phi_{4Q}$  in the SR for the pion DA appears to be enhanced relative to that for the  $\rho$ . This entails an increase of the  $\varphi_\pi$  moments  $\langle \xi^{2N} \rangle_\pi \geq \langle \xi^{2N} \rangle_{\rho_L} \geq \langle \xi^{2N} \rangle_{\text{Asy}}$ , as one sees from Table 1. Although the difference of the moments  $\langle \xi^6 \rangle_\pi - \langle \xi^6 \rangle_{\text{Asy}}$  is not very significant within the error bars, leading in turn to a comparatively small contribution of

the Gegenbauer coefficient  $a_6^\pi \approx 0.059 \sim 0$ , the associated uncertainties  $a_6^\pi \in [-0.297, 0.414]$  are quite large and comparable in magnitude with the result for the rho-meson:  $a_6^{\rho_L} = 0.05(73)$ .

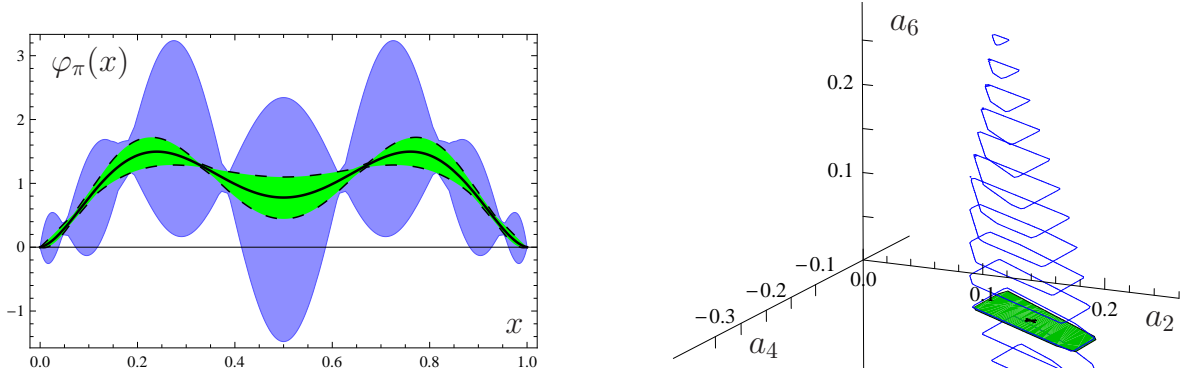


**Fig. 2** Left panel: Variation of the pion DA profiles for the 3D (blue oscillating wide band) and 2D (green narrow strip) models. Right panel: 3D graphics showing the pion DA “bunch” [29], obtained from QCD SRs with NLCs, in terms of the coefficients  $a_2, a_4, a_6$ , shown as a flight of “stairs” of slanted rectangles, while the original 2D BMS “bunch” [22] in the plane  $(a_2, a_4)$  is shown as a (green) shaded area, with the symbol **X** marking the BMS pion DA. All results have been obtained at the scale  $\mu^2 = 1 \text{ GeV}^2$ .

However, the inclusion of the  $a_6$  uncertainties in the model for the longitudinal rho meson is not improving its quality owing to the fact that the values of the lower coefficients  $a_2$  and  $a_4$ , within their region of validity, are already compatible with the asymptotic values. In contrast, in the pion case, one may try to extend the evaluation of the SRs in such a way as to include the effects of these large  $a_6$  uncertainties, amounting to a 3D analysis [29]. This is illustrated in Fig. 2. In the left panel, we show the profiles of the associated pion DAs expanded over  $a_2, a_4, a_6$  in the form of a 3D (blue) oscillating band bounded by solid lines in comparison with the original 2D band (narrower green strip bounded by broken lines) with the value  $a_6 = 0$  determined in [22]. The inclusion of  $a_6$  transforms the original 2D (green) slanted rectangle into a flight of “stairs” of (blue) slanted rectangles along the  $a_6$  axis (right panel).

### 3 Conclusions

We derived the profile of the leading-twist DA of the longitudinal  $\rho$  meson using QCD sum rules with nonlocal condensates along the lines of the analysis in [22] for the pion. We found that the longitudinal  $\rho$ -meson DA has a shape close to that obtained in the light-front quark model [15], bearing also a resemblance to the profile of a DA derived from the instanton liquid model [16]. From the point of view of the DA key characteristics, expressed via the inverse moment  $\langle x^{-1} \rangle_{\text{model}}$ , we found that the result obtained with QCD SRs with nonlocal condensates (Table 1) agrees, within the determined uncertainties, reasonably well with the value obtained with a model DA based on the first two Gegenbauer coefficients (Table 2). We also presented preliminary results on the transverse part of the  $\rho$ -meson, notably its decay constant and its moments  $\langle \xi^2 \rangle$  and  $\langle \xi^4 \rangle$ , using an improved sum rule relative to what was considered in [10; 11]. In contrast to the sum rules employed in [7; 8], our sum rule receives no contributions from the  $b_1$ -meson term or  $\rho$ -meson DAs of higher-twist. A full-fledged analysis of the  $\rho_T$  properties will be given elsewhere.

**Acknowledgements** The work of A.V.P. was supported by HadronPhysics2, Spanish Ministerio de Economía y Competitividad and EU FEDER under contract FPA2010-21750-C02-01, AIC10-D-000598, and GVPrometeo2009/129. A.V.P. thanks the organizers of the Light-Cone conference 2013 for financial support. We acknowledge support from the Heisenberg–Landau Program under Grant 2013 and the Russian Foundation for Fundamental Research (Grants No. 12-02-00613a and 11-01-00182a).

## References

1. Ball, P., Braun, V.M.: Use and misuse of QCD sum rules in heavy to light transitions: The Decay  $B \rightarrow \rho e$  neutrino reexamined. *Phys. Rev. D* **55**, 5561 (1997)
2. Ahmady, M., Sandapen, R.: Predicting  $\bar{B}^0 \rightarrow \rho^0 \gamma$  and  $\bar{B}_s^0 \rightarrow \rho \gamma$  using holographic AdS/QCD Distribution Amplitudes for the  $\rho$  meson. *Phys. Rev. D* **87**, 054013 (2013)
3. Forshaw, J., Sandapen, R.: An AdS/QCD holographic wavefunction for the rho meson and diffractive rho meson electroproduction. *Phys. Rev. Lett.* **109**, 081601 (2012)
4. Efremov, A.V., Radyushkin, A.V.: Factorization and asymptotic behaviour of pion form factor in QCD. *Phys. Lett. B* **94**, 245 (1980)
5. Lepage, G.P., Brodsky, S.J.: Exclusive processes in perturbative quantum chromodynamics. *Phys. Rev. D* **22**, 2157 (1980)
6. Mikhailov, S.V., Radyushkin, A.V.: Structure of two loop evolution kernels and evolution of the pion wave function in  $\phi^3$  in six-dimensions and QCD. *Nucl. Phys. B* **273**, 297 (1986)
7. Chernyak, V.L., Zhitnitsky, A.R.: Asymptotic behavior of exclusive processes in QCD. *Phys. Rept.* **112**, 173 (1984)
8. Ball, P., Braun, V.M.: The  $\rho$  Meson Light-Cone Distribution Amplitudes of Leading Twist Revisited. *Phys. Rev. D* **54**, 2182 (1996)
9. Bakulev, A.P., Mikhailov, S.V.: The  $\rho$ -meson and related meson wave functions in QCD sum rules with nonlocal condensates. *Phys. Lett. B* **436**, 351 (1998)
10. Bakulev, A.P., Mikhailov, S.V.: QCD vacuum tensor susceptibility and properties of transversely polarized mesons. *Eur. Phys. J. C* **17**, 129 (2000)
11. Bakulev, A.P., Mikhailov, S.V.: New shapes of light-cone distributions of the transversely polarized rho mesons. *Eur. Phys. J. C* **19**, 361 (2001)
12. Arthur, R., et al: Lattice Results for Low Moments of Light Meson Distribution Amplitudes. *Phys. Rev. D* **83**, 074505 (2011)
13. de Teramond, G.F., Brodsky, S.J.: Light-Front Holography: A First Approximation to QCD. *Phys. Rev. Lett.* **102**, 081601 (2009)
14. Vega, A., Schmidt, I., Branz, T., Gutsche, T., Lyubovitskij, V.E.: Meson wave function from holographic models. *Phys. Rev. D* **80**, 055014 (2009)
15. Choi, H.M., Ji, C.R.: Distribution amplitudes and decay constants for ( $\pi$ ,  $K$ ,  $\rho$ ,  $K^*$ ) mesons in light-front quark model. *Phys. Rev. D* **75**, 034019 (2007)
16. Dorokhov, A.E.: Distribution amplitudes of light mesons and photon in the instanton model. *Czech. J. Phys.* **56**, F169 (2006); *Braz. J. Phys.* **37**, 819 (2007)
17. Mikhailov, S.V., Radyushkin, A.V.: Quark condensate nonlocality and pion wave function in QCD. *Sov. J. Nucl. Phys.* **49**, 494 (1989)
18. Mikhailov, S.V., Radyushkin, A.V.: The pion wave function and QCD sum rules with nonlocal condensates. *Phys. Rev. D* **45**, 1754 (1992)
19. Bakulev, A.P., Mikhailov, S.V.: Lattice measurements of nonlocal quark condensates, vacuum correlation length, and pion distribution amplitude in QCD. *Phys. Rev. D* **65**, 114511 (2002)
20. Bakulev, A.P., Mikhailov, S.V., Stefanis, N.G.: CLEO and E791 data: A smoking gun for the pion distribution amplitude? *Phys. Lett. B* **578**, 91 (2004)
21. Mikhailov, S.V., Pimikov, A.V., Stefanis, N.G.: Endpoint behavior of the pion distribution amplitude in QCD sum rules with nonlocal condensates. *Phys. Rev. D* **82**, 054020 (2010)
22. Bakulev, A.P., Mikhailov, S.V., Stefanis, N.G.: QCD-based pion distribution amplitudes confronting experimental data. *Phys. Lett. B* **508**, 279 (2001); Erratum: *ibid.* **590**, 309 (2006)
23. Beringer, J., et al: Review of Particle Physics (RPP). *Phys. Rev. D* **86**, 010001 (2012)
24. Bakulev, A.P., Mikhailov, S.V., Stefanis, N.G.: Unbiased analysis of CLEO data beyond LO and pion distribution amplitude. *Phys. Rev. D* **67**, 074012 (2003)
25. Ball, P., Jones, G.: Twist-3 distribution amplitudes of  $K^*$  and  $\phi$  mesons. *JHEP* **0703**, 069 (2007)
26. Ioffe, B., Oganessian, A.: Valence quark distributions in mesons in generalized QCD sum rules. *Phys. Rev. D* **63**, 096006 (2001)
27. Oganessian, A., Samsonov, A.: Second moment of quark structure function of the rho meson in QCD sum rules. *JHEP* **0109**, 002 (2001)
28. Bakulev, A.P., Mikhailov, S.V., Stefanis, N.G.: Tagging the pion quark structure in QCD. *Phys. Rev. D* **73**, 056002 (2006)
29. Stefanis, N.G., Bakulev, A.P., Mikhailov, S.V., Pimikov, A.V.: Can We Understand an Auxetic Pion-Photon Transition Form Factor within QCD? *Phys. Rev. D* **87**, 094025 (2013)